Carrier Aggregation Compatible MIMO Antenna for LTE Handset

Kimmo Rasilainen[1, *], Anu Lehtovuori[1], Amine Boussada[2], and Ville Viikari[1]

Abstract—This paper proposes a two-element LTE MIMO handset antenna with physically different main and diversity antennas. The performance of the design is studied theoretically and experimentally. The investigated design utilises physically different main and diversity antennas to improve especially the low-band MIMO performance. A Combined Parasitic-coupled, Aperture-Matched (CPAM) antenna is used as the main antenna, and the diversity antenna is a simple Capacitive Coupling Element (CCE) design. The antenna covers the LTE bands from 698–960 MHz and 1710–2690 MHz with fixed matching circuits suitable for low-band (LB) Carrier Aggregation (CA). Measured total efficiency of the antennas is from -3 to -6 dB and -2 to -5 dB at the low and high bands, respectively. In the MIMO case, envelope correlation coefficient (ECC) and multiplexing efficiency ($\tilde{\eta}_{\mathrm{mux}}$) are studied also from measurements.

1. INTRODUCTION

In both current Long Term Evolution Advanced (LTE-A) and upcoming fifth-generation (5G) wireless communication systems, one of the main trends is going for higher and higher data rates [1]. Accomplishing this requires utilising more advanced antenna designs. Solutions include the use of higher-order Multiple-Input, Multiple-Output (MIMO) technology, in which several antennas are used for simultaneous communication. Alternatively, one can use several simultaneous component carriers (CC) for communication in Carrier Aggregation (CA) technology [2, 3]. These CCs can be either within one frequency band (intra-band CA) or spread across different bands (inter-band CA).

Implementing MIMO means increasing the number of antennas within the limited volume available in current handsets. One solution to this issue is to use smaller antennas with tunable matching circuits [4–6]. With frequency tuning, antenna size can be reduced as the entire frequency band of a given radio system is not covered instantaneously. By changing the state of the tunable component (typically, a capacitor), the targeted frequency band is covered in narrower segments. In this approach, finding a well-performing matching circuit is important, as well as the fact that the tunable component causes additional losses compared to fully passive implementations. The use of tunable components is challenging for CA, which typically benefits from a passive design. This relates to losses and also to potential nonlinearities in the tuning components: they can generate harmonic frequencies that occur at the transmitting (Tx) or receiving (Rx) frequencies with certain CC combinations. Their effects need to be properly taken into account in RF front-end design.

Recent multi-element handset antenna designs can be found in, e.g., [7–10]. The design presented in [7] implements a four-element MIMO antenna for the low band (LB) (698–960 MHz), but the study does not consider high band (HB) MIMO. On the other hand, the work of [8] features both LB and HB MIMO, and different frequency bands starting from the 800-MHz range are covered using a diode switch.

In this work, we consider a design that conforms with the requirements of MIMO and CA at both LB and HB, and also covers all of the LTE-A LB. The proposed two-element implementation utilises two physically different radiators as the main and diversity antennas with fully passive matching networks. The main antenna features a combination of aperture-matched, fed, and parasitic radiators, and in the current work it is referred to as a Combined Parasitic-coupled, Aperture-Matched (CPAM) antenna. A more conventional, simple Capacitive Coupling Element (CCE) [11, 12] is used as the diversity antenna. The CPAM antenna is based on a recent design presented in [13], and the design of this work is significantly simpler and more straightforward compared to the previous work; both the number of matching components and feeds have been reduced by 50%. The current study looks at the two-element antenna also for its actual MIMO performance, which is investigated using both simulation and experimental results.

2. ANTENNA AND MATCHING CIRCUIT DESIGN

The approach considered in this work utilises antennas that are placed around or near the edge of the device to maximise the antenna volume while occupying a relatively low surface area. Figure 1 illustrates the proposed main and diversity antennas. All of the antennas are designed for a 0.8-mm thick FR-4 substrate ($\varepsilon_r = 4.4$), and handset dimensions of $160 \times 80 \times 5\,\text{mm}^3$ [length × width × thickness] are considered. These dimensions are comparable to today's high-end smartphones, e.g., the iPhone 6 Plus by Apple. In this study, electromagnetic simulations of the antennas are performed in the CST Microwave Studio software [14], and circuit simulations are carried out in Optenni Lab [15].

The matching circuits of Figure 2 are implemented using GQM18 capacitors and LQW18 inductors from Murata, and simulations use S-parameter models for them available from the manufacturer. The matching components are placed on the chassis using a suitable networks of pads, and their effect is also taken into account in the simulations.

2.1. Main Antenna Utilising Combined Aperture Matching and Parasitic Coupler (CPAM)

Figure 1 shows the geometry and dimensions of the proposed CPAM main antenna, and the corresponding matching circuit is illustrated in Figure 2. The current study aims at achieving good performance in terms of instantaneous bandwidth and efficiency also at the LB with as simple a design as possible. This applies both to the number of feed ports and matching components needed to implement the desired performance.

To get a well-performing design, the antenna structure and circuits are co-optimised using CST and Optenni Lab. As a starting point, the overall device thickness was fixed to 5 mm to have a sufficiently low-profile design. For the antennas, the length of the elements along the sides of the device, the position of the gap between the corner-located L-shaped elements, as well as the size and location of the
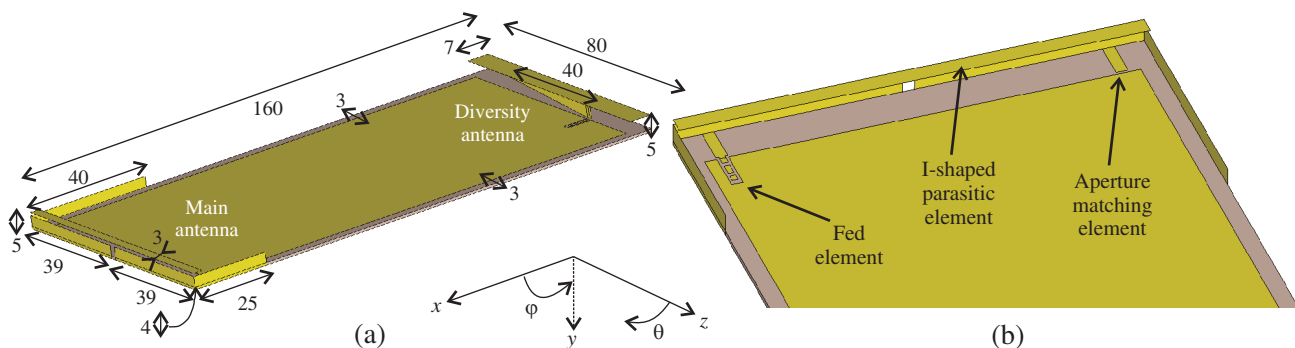

Figure 1. Illustration of (a) the proposed CPAM main and CCE diversity antennas and (b) close-up of the different active, parasitic, and aperture-matched elements in the CPAM antenna. All dimensions are in mm.
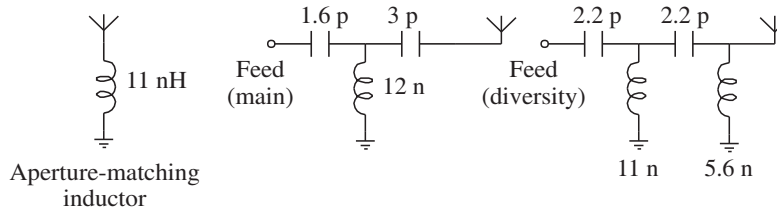
Figure 2. Matching circuits used in the CPAM main and CCE diversity antennas in simulations and measurements. The circuits are implemented using actual Murata capacitors and inductors.

parasitic I-element were modified during the optimisation. On the circuit side, the number of matching components allowed per each radiator was at most four. The design goal was to achieve an embedded radiation efficiency [16] better than 80% at LB (698–960 MHz) and better than 60% at HB (1710–2690 MHz). By varying one parameter at a time (different antenna dimensions or circuit properties), a suitable antenna and circuit combination was found with a relatively low number of iterations.

For the final main antenna design, the ground clearance is 7 mm and 3 mm along the chassis ends and sides, respectively. The 7-mm clearance in the ends is applied symmetrically in both ends, and the value is a suitable compromise between antenna performance and overall volume. With this approach, it is possible to cover both LB and HB with a single feed, and the number of circuit components has reduced to four. A three-element high-pass type network is used to match the fed L-shaped antenna at the desired bands, and an inductor is used for aperture matching in the other L-element. Figure 1(b) shows details of the different main antenna parts.

Comparing the current CPAM antenna to the previously-presented design of [13], the solution investigated here has many significant benefits over the earlier one. Even though both designs are conceptually related, the one shown in Figure 1 is easier to implement in practice. Altogether four lumped components (three for the active antenna, one for aperture matching) are needed in the CPAM antenna whereas the design of [13] has two separate feeds and eight matching components. The fully-parasitic I-shaped metal strip ($80 \times 3\,\text{mm}^2$) positioned 1 mm above the edge of the L-shaped antennas is simpler than the coupler grounded through an inductor in [13]. The parasitic element couples to the L-shaped corner elements, thereby increasing the effective antenna size. Together with changes in antenna impedance, this results in improved low-band performance. A low-permittivity spacer is used to maintain a proper placement of the I-element. The overall dimensions of the CPAM antenna are smaller than those of [13], which makes it easier to place the antennas in the handset.

Having fewer circuit components and antenna feeds in the design is a desirable feature. This is due
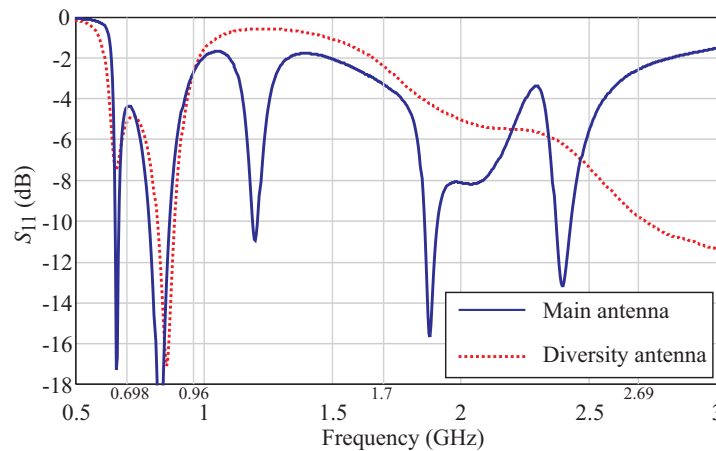

Figure 3. Simulated impedance matching of the CPAM main and CCE diversity antennas in the single-ended case.

to the fact that less components typically results in lower total losses, and using a single feed instead of two separate ones can both reduce the amount of RF hardware needed and also simplify the design of the RF front-end. Figure 3 presents the input matching of the proposed CPAM antenna in the single-antenna case. The results show that the current design instantaneously covers the LTE low band with a fully fixed matching network. This is beneficial for using this antenna for CA applications.

2.2. Capacitive-Coupling-Element Diversity Antenna

When designing small antennas for handsets, larger antennas are better. This somewhat paradoxical statement results from the fact that the lowest operating frequencies benefit from a large antenna volume and are still the most challenging ones to implement despite consuming the largest overall size. For this reason, we begin designing the diversity CCE antenna using a traditional design flow presented in [17], wherein the implementation starts from the low-band case. The available overall volume ($7 \times 80 \times 4.2 \, \text{mm}^3$) is used efficiently with a coupling element that is as large and as simple as possible.

As the next step, a matching circuit is added to the antenna for implementing the desired frequency bands. A high-pass type circuit (see Figure 2) is needed to allow for proper high-band operation. Using four components was found to be sufficient to make the antenna operate well at the low band. Finally, an additional triangular tapering is added to the feeding strip of the diversity antenna to further improve the high-band performance, as introduced in [17]. Figure 3 shows the matching of the diversity antenna after the aforementioned design steps.

Regarding practical antenna designs (e.g., in commercial implementations), the main performance metric to consider is the (total) efficiency rather than impedance matching [18]. Therefore, the antennas and matching circuits proposed in this work are designed 'efficiency first', with the goal of emphasising the efficiency performance in both the single- and multi-antenna cases.

3. PERFORMANCE OF THE MAIN AND DIVERSITY ANTENNAS IN THE MIMO CASE

In this section, the proposed antenna is investigated computationally and experimentally in terms of S-parameters (input matching and mutual coupling), efficiency, and multiantenna (MIMO) characteristics. Particular emphasis is placed on careful and realistic MIMO characterisation. Figure 4 shows the measurement setup used to characterise the antenna efficiency and MIMO performance.
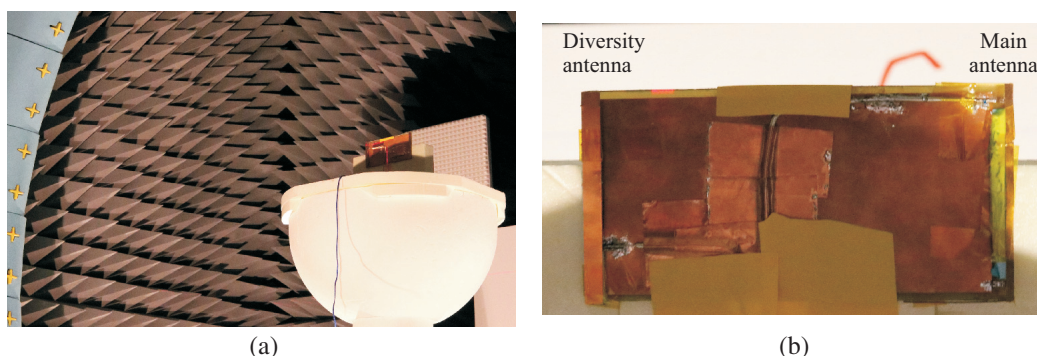

Figure 4. (a) Photograph of the measurement setup (Satimo Stargate) used to characterise antenna efficiency and fields. (b) Close-up of the antenna prototype in the measurement chamber.

3.1. Impedance Matching and Mutual Coupling

Figure 5 gives the simulated and measured S-parameters of the main and diversity antennas in the two-element MIMO case. In the figure, ports 1 and 2 refer to the main and diversity antennas, respectively. At LB, the input matching results of the antennas are in good agreement in simulations and
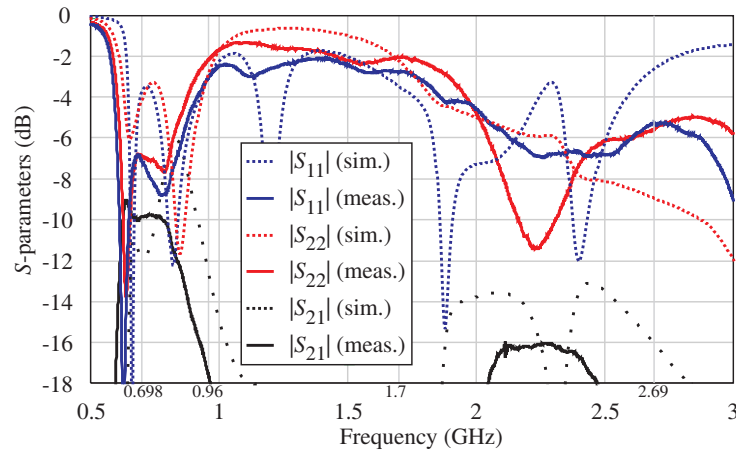
Figure 5. Simulated and measured scattering parameters in the MIMO case. Port 1 = CPAM main antenna. Port 2 = CCE diversity antenna.

measurements, respectively, but there are some discrepancies between the calculated and experimental results. At higher frequencies, the results have more variance between the two antennas. The differences in the results are mainly due to the sensitivity of the main and diversity antennas to the placement of the parasitic I-element and CCE, respectively.

At LB, the measured mutual coupling is better than -10 dB between the main and diversity antennas, which is a suitable level for practical MIMO implementations. During the design, the aim was to achieve a mutual coupling level from -8 to -10 dB. This is a practically feasible value, as the level of mutual coupling should typically be from -6 to -10 dB or better [19–22]. Compared to [13], where identical main and diversity antennas are used, the mutual coupling has reduced at LB. This means that the 'challenging' low-band performance can benefit from the use of physical antenna diversity. At HB, the mutual coupling remains low.

3.2. Antenna Efficiency

Figure 6 gives the simulated radiation (η_{rad}) and total (η_{tot}) efficiency of the main and diversity antennas in the single-ended case. When calculating the efficiencies from simulations, realistic losses are assumed both for the materials (conductor and dielectric losses) and for the matching components. The curves show that for both antennas, the η_{rad} performance is very good at both LB and HB. Within the targeted LTE bands (698–960 MHz and 1700–2690 MHz), the η_{tot} is better than -4 dB.

Figure 7 illustrates the simulated and measured efficiency in the MIMO case. Going from single-ended to multi-antenna case decreases the average η_{tot} of the diversity antenna only around 1 dB at LB, whereas the drop is more significant for the main antenna. At HB, on the other hand, the η_{tot} of the main antenna is less affected than that of the diversity antenna from including MIMO operation.

Decreasing low-band efficiency is an expected result, as at frequencies below 1 GHz, the chassis contributes the most to overall handset radiation [12]. In the current design, the main and diversity antennas both couple to the same chassis, and this coupling reduces efficiency. Similar behaviour was observed also in [13]. For the high-band case, the η_{tot} is mainly affected by the matching, as for both antennas, adding the diversity antenna has only small effect on η_{rad}.

The efficiency performances of the proposed main and diversity antennas can be compared to some of the MIMO handset antennas presented in recent literature [7, 8, 23, 24]. For the four-element MIMO design given in [7], the measured efficiency is from -2.2 to -4 dB at the low band, but no HB results are given. In [23], both LB and HB MIMO are considered, and the LB efficiency is up to -4 dB, and HB efficiency is from -1.5 to -3 dB.

Examples of MIMO antennas with tunable matching circuits are given in, e.g., [8, 24]. The two-element design of [8] achieves an efficiency of -1.5 to -4 dB at both LB and HB. However, as mentioned previously, the LB starts only from the 800-MHz range, meaning that the most challenging LTE LB
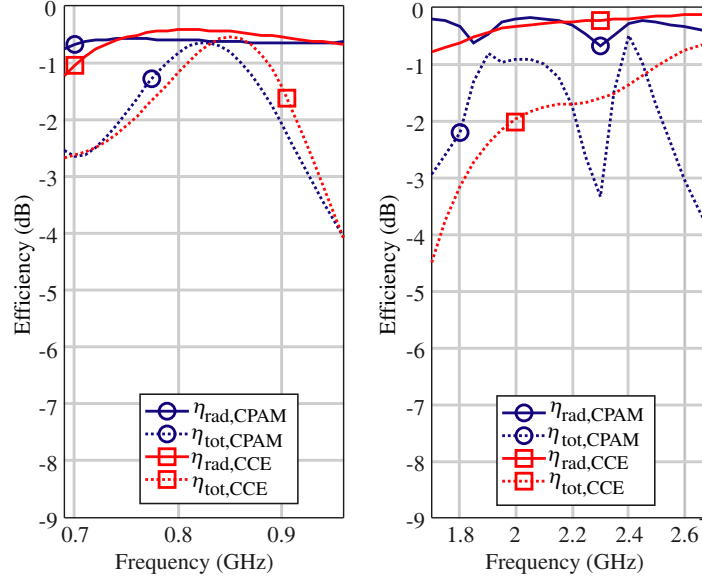
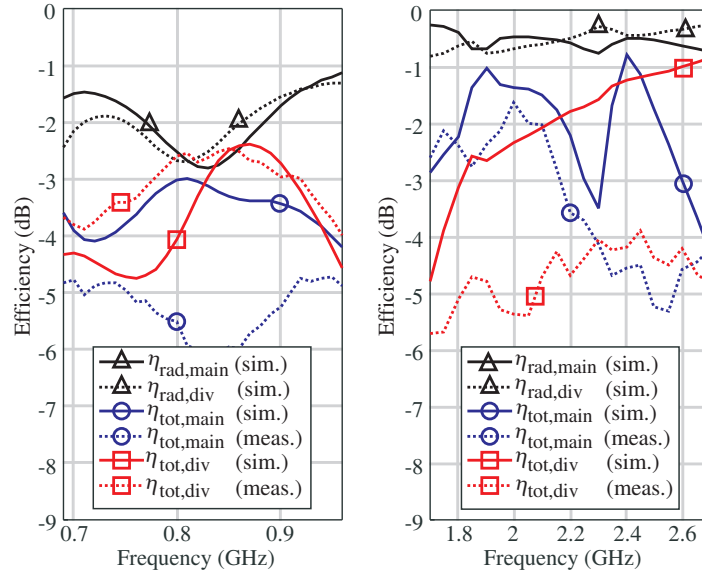**Figure 6.** Simulated efficiency of the CPAM main and CCE diversity antennas in the single-ended case.

Figure 7. Simulated and measured antenna efficiency in the MIMO case.

frequencies are missing even with tuning. In [24], identical main and diversity antennas with a digitally-tunable capacitor (DTC) are used in the same end of the device. With this approach, the efficiency is better than $-3\,\text{dB}$ at LB and HB, but one drawback is the need for a tunable matching circuit. With respect to the results mentioned above, the efficiency performance obtained in this work is good (see Figure 7), especially in light of the less-than-optimal matching levels.

3.3. Multi-Antenna Characteristics

When considering the suitability of the proposed design for actual multi-antenna applications, certain MIMO parameters and quantities need to be analysed. In this work, the MIMO performance is characterised in terms of envelope correlation coefficient (ECC) [16, 25], and multiplexing efficiency ($\tilde{\eta}_{\text{mux}}$) [26]. The ECC is a measure of how similar the radiation patterns of the two antennas are. A
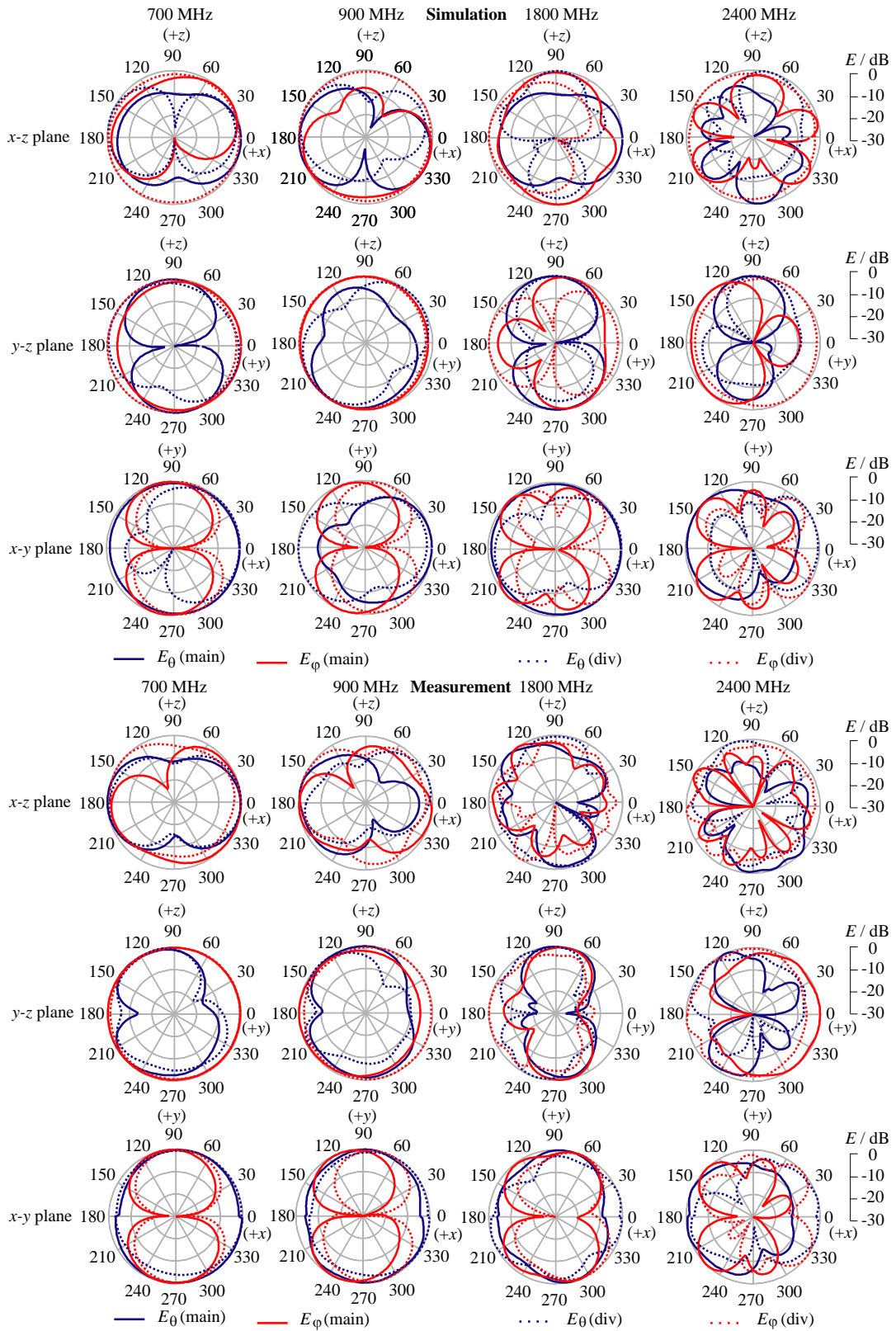
Figure 8. Simulated and measured radiation patterns of the main and diversity antennas at 700 MHz, 900 MHz, 1800 MHz, and 2400 MHz.

general guideline is that ECC values of $\rho_e < 0.5$ are typically desired to make efficient use of diversity techniques. Multiplexing efficiency is a computationally simple metric that describes the loss of signal-to-noise ratio (SNR) with respect to ideal MIMO antennas due to antenna efficiency, efficiency imbalance, and correlation in a particular multi-antenna implementation [26].

It is possible to calculate the ECC either from antenna far fields or from S-parameters [16, 27]. The previous approach is laborious, especially across wide frequency ranges, whereas the latter one is simple and fast to use. For this reason, many publications use the formula based on S-parameters to calculate the ECC (e.g., [23, 28, 29]). The problem related to characterising the ECC from simulated and/or measured S-parameters is that the formulas used in the calculations are strictly valid for antennas without Ohmic losses [16], but as mentioned in [29], they are a sufficient approximation for antennas with high efficiency. In a more general case, this method typically results in too optimistic ECC values, especially at LB. Thus, in this work we calculate the ECC from simulated and measured fields, assuming an isotropic and reflection-rich environment. Figure 8 visualises the simulated and measured (normalised) fields at 700, 900, 1800, and 2400 MHz, and losses due to impedance matching are taken into account in the results. The patterns show that at the low band, the radiation patterns of the main and diversity antennas are more similar than at the high band.

Figure 9 presents the simulated and measured ECC and $\tilde{\eta}_{\mathrm{mux}}$ values. According to simulations, the LB ECC is rather large, but the measured ρ_e drops below the threshold above 850 MHz. Considering LB handset antennas, the achieved ECC values are typical, especially when calculating them from the radiation patterns. At HB, the simulated and measured correlation values are well below the threshold. Studies on the ECC performance of identical CPAM antennas have shown ECC values of up to 0.9 at LB. Thus, the proposed design approach can improve also the LB MIMO performance.

The $\tilde{\eta}_{\mathrm{mux}}$ results of Figure 9 show that at LB, the average multiplexing efficiency is from -5 to $-7\,\mathrm{dB}$ in both simulations and measurements. At the high band, both the simulated and measured ρ_e values are low. This means that, as per the formula given in [26], the $\tilde{\eta}_{\mathrm{mux}}$ converges to the mean of individual antenna efficiencies (in dB scale), and the lower efficiency largely determines the total $\tilde{\eta}_{\mathrm{mux}}$ performance. With the proposed antenna design, the simulated and measured multiplexing efficiencies are approximately -2 to $-3\,\mathrm{dB}$ and $-4\,\mathrm{dB}$, respectively at HB. The obtained $\tilde{\eta}_{\mathrm{mux}}$ values are comparable to or even better than those achieved in [24], especially at LB.

When considering the proposed antennas in an actual device with all the electronics, the ρ_e values probably decrease, which is promising for applying diversity techniques for the current antennas. One ECC-related challenge, especially at LB, is that the main and diversity antennas now radiate more or
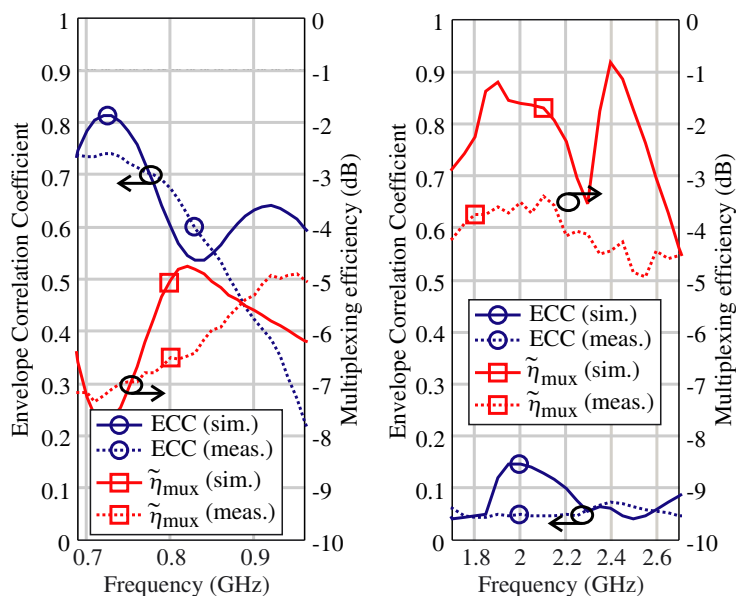

Figure 9. Calculated and measured envelope correlation coefficient (ECC) and multiplexing efficiency ($\tilde{\eta}_{\mathrm{mux}}$) performance.

less the same way (see Figure 8), leading to inherently 'high' ECC. A solution could be to use, e.g., capacitive main and inductive diversity antennas to get even greater benefit from physical antenna diversity, or to find suitable antenna and feed locations using the theory of characteristic modes [9]. Exciting the main and diversity antennas through different (ideally, orthogonal) chassis wavemodes reduces the antenna correlation.

4. CONCLUSION

In this work, the performance of a two-element LTE MIMO handset antenna is presented. By combining two physically different antenna elements and a fixed matching network, the proposed simple diversity antenna covers the LTE low-band with total efficiency better than $-4\,\mathrm{dB}$. Measured MIMO characteristics show ECC values typical for this type of device without any decoupling techniques. The fully passive implementation and good instantaneous bandwidth coverage makes the current design a potential candidate for intra-band CA applications.

ACKNOWLEDGMENT

REFERENCES

1. Hossain, E. and M. Hasan, "5G cellular: Key enabling technologies and research challenges," *IEEE Instrum. Meas. Mag.*, Vol. 18, No. 3, 11–21, Jun. 2015.
2. Bassam, S. A., W. Chen, M. Helaoui, and F. M. Ghannouchi, "Transmitter architecture for CA: Carrier aggregation in LTE-Advanced systems," *IEEE Microw. Mag.*, Vol. 14, No. 5, 78–86, Jul./Aug. 2013.
3. Valkonen, R., A. Lehtovuori, and C. Icheln, "Dual-feed, single-CCE antenna facilitating inter-band carrier aggregation in LTE-A handsets," *2013 7th European Conference on Antennas and Propagation (EuCAP)*, 3954–3958, Gothenburg, Sweden, Apr. 2013.
4. Yoon, C., S.-G. Hwang, G.-C. Lee, W.-S. Kim, H.-C. Lee, C.-H. Lee, and H.-D. Park, "A frequency-selecting technique for mobile handset antennas based on capacitance switching," *Progress In Electromagnetics Research*, Vol. 138, 99–113, 2013.
5. Ali, S. M. and K. Payandejoo, "Tunable antenna techniques for compact handset applications," *IET Microw. Antennas Propag.*, Vol. 8, No. 6, 401–408, Apr. 2014.
6. Caporal del Barrio, S., A. Morris, and G. F. Pedersen, "Addressing carrier aggregation with narrow-band tunable antennas," *2016 10th European Conference on Antennas and Propagation (EuCAP)*, 1–5, Davos, Switzerland, Apr. 2016.
7. Wong, K.-L., Y.-C. Chen, and W.-Y. Li, "Four LTE low-band smartphone antennas and their MIMO performance with user's hand presence," *Microw. Optical Technol. Lett.*, Vol. 58, No. 9, 2046–2052, Sep. 2016.
8. Ban, Y.-L, Y.-F. Qiang, G. Wu, H. Wang, and K.-L. Wong, "Reconfigurable narrow-frame antenna for LTE/WWAN metal-rimmed smartphone applications," *IET Microw. Antennas Propag.*, Vol. 10, No. 10, 1092–1100, Jul. 2016.
9. Li, H., Z. T. Miers, and B. K. Lau, "Design of orthogonal MIMO handset antennas based on characteristic mode manipulation at frequency bands below 1 GHz," *IEEE Trans. Antennas Propag.*, Vol. 62, No. 5, 2756–2766, May 2014.

10. Wi, H., B. Kim, W. Jung, and B. Lee, "Multiband handset antenna analysis including LTE band MIMO service," *Progress In Electromagnetics Research*, Vol. 138, 661–673, 2013.

11. Villanen, J., J. Ollikainen, O. Kivekäs, and P. Vainikainen, "Coupling element based mobile terminal antenna structures," *IEEE Trans. Antennas Propag.*, Vol. 54, No. 7, 2142–2153, Jul. 2006.

12. Vainikainen, P., J. Ollikainen, O. Kivekäs, and I. Kelander, "Resonator-based analysis of the combination of mobile handset antenna and chassis," *IEEE Trans. Antennas Propag.*, Vol. 50, No. 10, 1433–1444, Oct. 2002.

13. Rasilainen, K., A. Lehtovuori, and V. Viikari, "LTE handset antenna with closely-located radiators, low-band MIMO, and high efficiency," *2017 11th European Conference on Antennas and Propagation (EuCAP)*, 3074–3078, Paris, France, Mar. 2017.

14. CST Microwave Studio, an FDTD/FIT based electromagnetic simulator, version 2013, CST AG, Darmstadt, Germany, [Online], Available: http://www.cst.com (Cited Jun. 8, 2017).

15. Optenni Lab, matching circuit generation and antenna analysis software, ver. 3.3, Optenni Ltd., Espoo, Finland, [Online], Available: http://www.optenni.com (Cited Jun. 8, 2017).

16. Kildal, P.-S., *Foundations of Antenna Engineering: A Unified Approach for Line-of-Sight and Multipath*, Kildal, 2015.

17. Ilvonen, J., R. Valkonen, J. Holopainen, and V. Viikari, "Design strategy for 4G handset antenna and a multiband hybrid antenna," *IEEE Trans. Antennas Propag.*, Vol. 62, No. 4, 1918–1927, Apr. 2014.

18. Lehtovuori, A., J. Ilvonen, K. Rasilainen, and V. Viikari, "Single-element handset antenna design for modern smartphones: An industrial approach," *2017 11th European Conference on Antennas and Propagation (EuCAP)*, 2960–2963, Paris, France, Mar. 2017.

19. Ilvonen, J., J. Holopainen, K. Rasilainen, A. Lehtovuori, and V. Viikari, "Suitable multiantenna placement in mobile handsets based on electromagnetic isolation," *2016 10th European Conference on Antennas and Propagation (EuCAP)*, 1–4, Davos, Switzerland, Apr. 2016.

20. Wong, K.-L., T.-W. Kang, and M.-F. Tu, "Internal mobile phone antenna array for LTE/WWAN and LTE MIMO operations," *Microw. Optical Technol. Lett.*, Vol. 53, No. 7, 1569–1573, Jul. 2011.

21. Cihangir, A., F. Ferrero, G. Jacquemod, P. Brachat, and C. Luxey, "Neutralized coupling elemets for MIMO operation in 4G mobile terminals," *IEEE Antennas Wireless Propag. Lett.*, Vol. 13, 141–144, 2014.

22. Zhang, S., K. Zhao, Z. Ying, and S. He, "Adaptive quad-element multi-wideband antenna array for user-effective LTE MIMO mobile terminals," *IEEE Trans. Antennas Propag.*, Vol. 61, No. 8, 4275–4283, Aug. 2013.

23. Li, K., Y. Shi, and C.-H. Liang, "Quad-element multi-band antenna array in the smart mobile phone for LTE MIMO operations," *Microw. Opt. Technol. Lett.*, Vol. 58, No. 11, 2619–2626, Nov. 2016.

24. Ilvonen, J., R. Valkonen, J. Holopainen, and V. Viikari, "Multiband frequency reconfigurable 4G handset antenna with MIMO capability," *Progress In Electromagnetics Research*, Vol. 148, 233–243, 2014.

25. Vaughan, R. G. and J. Bach Andersen, "Antenna diversity in mobile communications," *IEEE Trans. Veh. Commun.*, Vol. VT-36, No. 4, 149–172, Nov. 1987.

26. Tian, R., B. K. Lau, and Z. Ying, "Multiplexing efficiency of MIMO antennas," *IEEE Antennas Wireless Propag. Lett.*, Vol. 10, 183–186, 2011.

27. Blanch, S., J. Romeu, and I. Corbella, "Exact representation of antenna system diversity performance from input parameter description," *Electron. Lett.*, Vol. 39, No. 9, 705–707, May 2003.

28. Shoaib, S., I. Shoaib, X. Chen, and C. G. Parini, "MIMO antennas for next generation mobile terminals," *2016 10th European Conference on Antennas and Propagation (EuCAP)*, 1–4, Davos, Switzerland, Apr. 2016.

29. Chamok, N. H., M. H. Yilmaz, H. Arslan, and M. Ali, "High-gain pattern reconfigurable MIMO antenna array for wireless handheld terminals," *IEEE Trans. Antennas Propag.*, Vol. 64, No. 10, 4306–4315, Oct. 2016.